

A New Perspective on Drawing Venn Diagrams for Data Visualization

Bálint Csanády

Institute of Mathematics, ELTE Eötvös Loránd University, Budapest, Hungary

Abstract

We introduce *VennFan*, a method for generating n -set Venn diagrams based on the polar coordinate projection of trigonometric boundaries, resulting in Venn diagrams that resemble a set of fan blades. Unlike most classical constructions, our method emphasizes readability and customizability by using shaped sinusoids and amplitude scaling. We describe both sine- and cosine-based variants of *VennFan* and propose an automatic label placement heuristic tailored to these fan-like layouts. *VennFan* is available as a Python package¹.

1 Introduction

Venn diagrams visualize all possible logical relations between n sets. For $n < 6$, they can be realized by overlapping ellipses (Figure 1) [14, 10]. Using Euler’s formula together with the fact that two ellipses can meet in at most four points, Grünbaum showed that no Venn diagram with six or more sets can be drawn using ellipses [8]. Therefore, due to the exponential nature of Venn diagrams, the readability of known constructions deteriorates rapidly as n increases beyond 5.

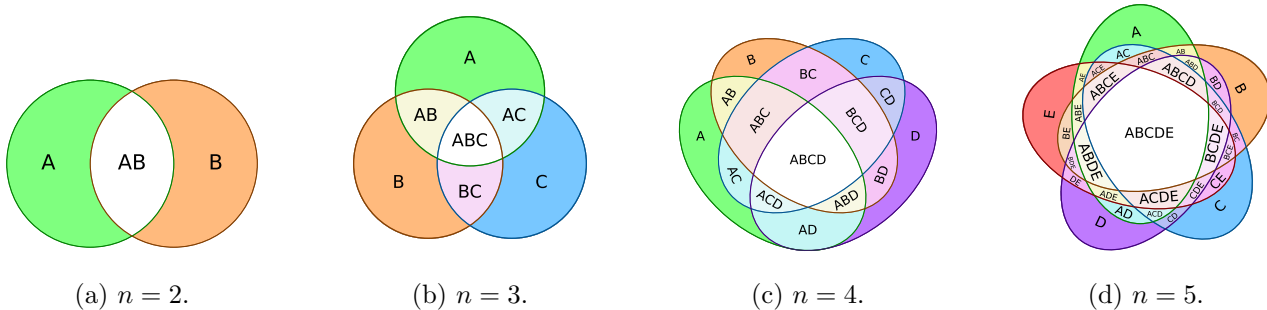
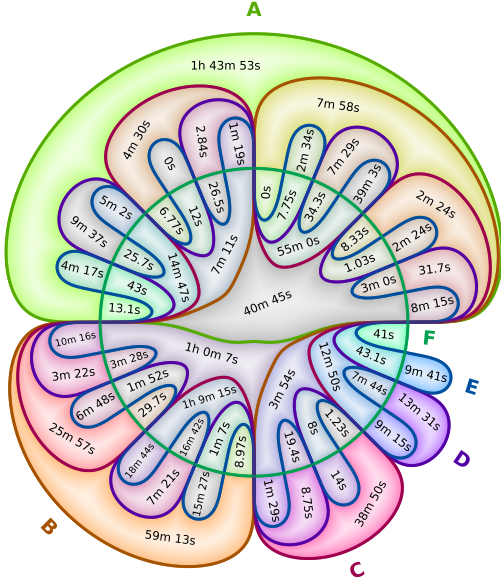


Figure 1: Ellipsoidal Venn diagrams for $2 \leq n \leq 5$.

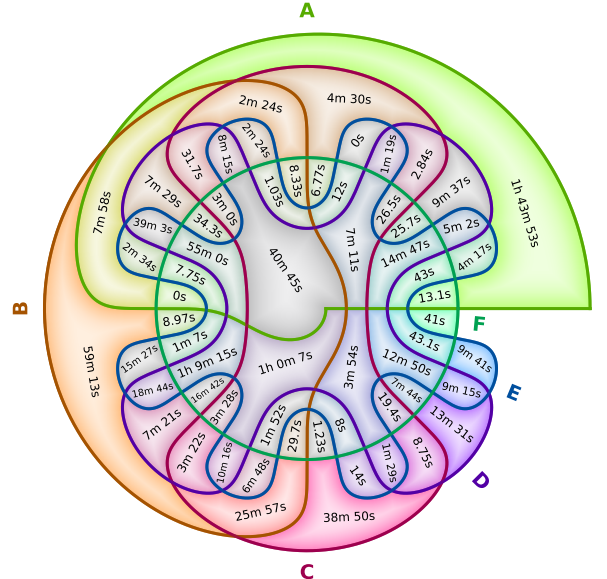
The challenge is not only to ensure topological completeness (that all 2^n intersections are represented), but also to support the presentation of data in a form that remains interpretable. Ultimately, what counts as “readable” is subjective and up to personal preference. Consequently, several additional constraints on Venn diagrams have been proposed with the implicit goal of improving readability. These constraints lead to interesting combinatorial and geometric problems in their own right, and deserve attention independently of their effectiveness for data visualization.

In this work however, we argue that relaxing most of these constraints allows the construction of Venn diagrams that are, in many situations, better suited for presenting data. One domain where such data naturally arises, and where Venn diagrams may be particularly useful, is biology and medicine. For time series data annotated by multiple experts, one may be interested in the overlap structure between the different sets of annotations. For example, annotations may come from several human experts (e.g., clinicians) or from automated detection software that mark abnormalities within the data, such as epileptic seizures in EEG recordings. Our construction, *VennFan*, provides a flexible method for representing such information with clearly readable labels and visually distinct classes (Figure 2).

¹<https://pypi.org/project/vennfan/>



(a) Sine-based.



(b) Cosine-based.

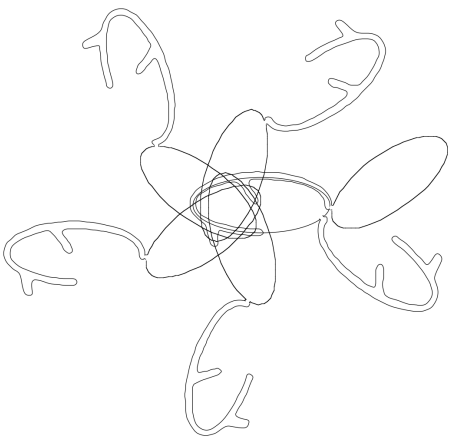
Figure 2: *VennFan* diagrams of overlaps between six different seizure annotators in EEG data.

2 Background

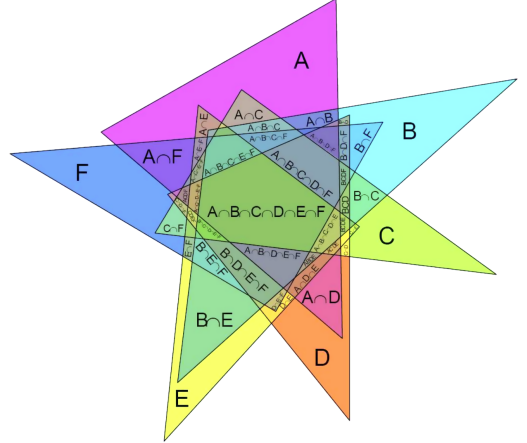
Following Grünbaum and Ruskey [10, 12], let $C = \{C_0, \dots, C_{n-1}\}$ be a family of simple closed curves in the plane, each representing one of n sets. For each i , let X_i denote either the bounded interior or the unbounded exterior of C_i . We call C an *independent family* if every one of the 2^n intersections

$$X_0 \cap X_1 \cap \dots \cap X_{n-1}$$

is non-empty. Each connected component of such an intersection is called a *region*. If every one of the 2^n intersections consists of a single region, we call the independent family a *Venn diagram*. A Venn diagram is called *simple* if at most two boundaries meet at any point [1].



(a) Grünbaum's nice diagram.



(b) Carroll's simple triangle diagram.

Figure 3: Nice and simple Venn diagrams for $n = 6$.

A natural requirement motivated by the $n \leq 5$ ellipsoidal constructions would be to represent all of the curves by congruent shapes; such diagrams are called *nice* [9] or *congruent* [12] (Figure 3a). Another natural way to generalize is to keep the shapes as elementary as possible: for $n = 6$ it is feasible to draw a simple Venn diagram using triangles. Figure 3b shows Carroll's construction found by computer search [2]. The ultimate marriage for these two ideas — a Venn diagram on six sets drawn

with congruent equilateral triangles — appears to remain open [12, 10]. Although these conditions are easily motivated by looking at the familiar diagrams for $n \leq 5$, their success in the quest for readable data visualizations is debatable.

An elegant general Venn-like construction for arbitrary n uses trigonometric curves; it goes back to ideas of C. A. B. Smith and was later discussed by Edwards [4, 12]. In this classical construction,

$$f_i(x) = \sin(2^i x)/2^i, \quad x \in [-\pi, \pi], \quad i = 0, 1, \dots, n-1, \quad (1)$$

the amplitude decays exponentially with i , and when it is drawn as a graph in the plane the boundaries are not closed curves, so they do not form a planar Venn diagram in the usual sense (Figure 4a). Both of these issues are addressed by *VennFan*, which is inspired by Smith’s construction.

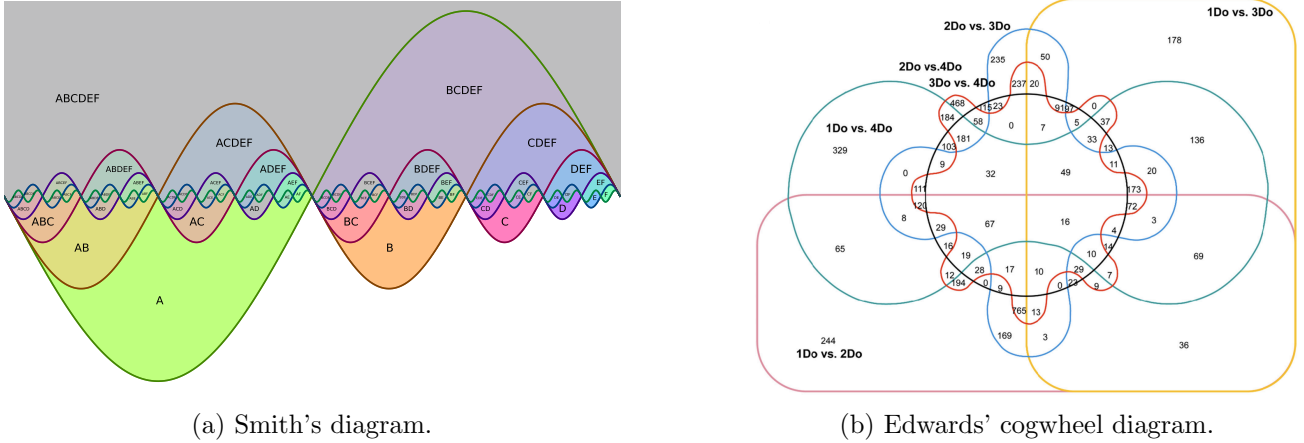


Figure 4: Examples of trigonometric (Smith) and cogwheel (Edwards) diagrams.

Finally, a particularly influential way of drawing Venn diagrams for $n > 5$ is the spherical construction pioneered by Edwards [3, 4], which yields his well-known *cogwheel* diagrams after projection to the plane. His design, although arguably the state-of-the-art option for representing data, also suffers from a rapid decrease of region sizes as n grows, and its planar appearance can look somewhat arbitrary at first glance. Figure 4b shows an example of cogwheel diagrams being used to represent gene expressions by Yuan et al. [16]. As we will see, the cosine-based version of *VennFan* is topologically equivalent to Edwards’ construction, and thus offers an alternative, more tunable way to realize the same combinatorial structure.

3 The *VennFan* Construction

The first step is to overcome the exponential amplitude decay present in Smith’s construction. For example, instead of exponential amplitude decay, we can introduce linear decay $\lambda(i) = \frac{n-1-i}{n}$. However, if we do this, the curves will collide (Figure 5a). To mitigate these collisions, we *shape* the curves by raising them to a power with exponent $p < 1$, leading to Equation 2:

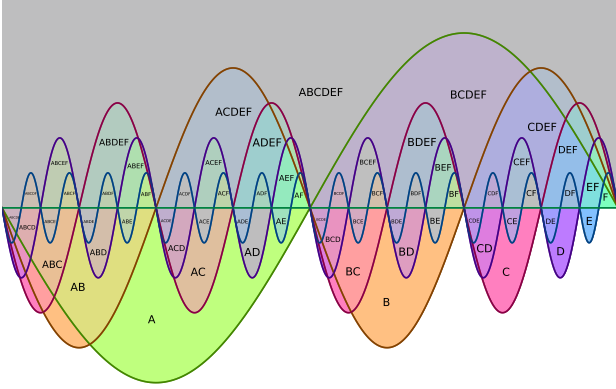
$$f_i(x) = \lambda(i) \operatorname{sgn}(\sin(2^i x)) |\sin(2^i x)|^p, \quad x \in [-\pi, \pi], \quad i = 0, \dots, n-1. \quad (2)$$

Note, that as we decrease $p < 1$ the shape of the sine waves become “fatter” (Figure 5b), with $p \rightarrow 0$ tending to a square wave.

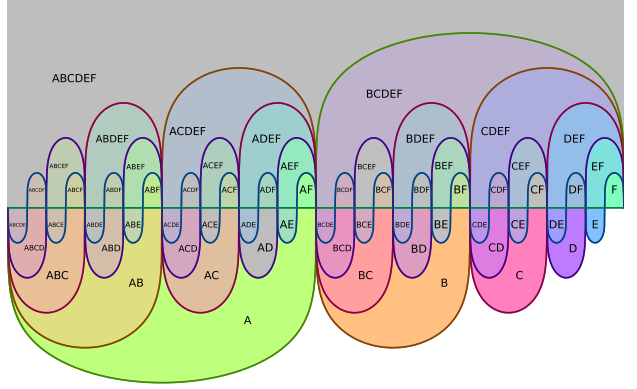
The second step is to turn the unbounded outer region into a bounded one and to convert the boundaries into simple closed curves. We achieve this by projecting the rectangle $[-\pi, \pi] \times [-1, 1]$ onto the unit disc by treating x as the polar angle ϑ and $f_i(x)$ as a radial deviation from radius 1 (Figure 6a). More precisely, we draw the parametric curve:

$$g_i(\vartheta) = ((1 + f_i(\vartheta)) \cos \vartheta, (1 + f_i(\vartheta)) \sin \vartheta), \quad \vartheta \in [-\pi, \pi], \quad i = 0, \dots, n-1. \quad (3)$$

Notice that $|f_i(\vartheta)| < 1$, which prevents $g_i(\vartheta)$ from passing through the origin.



(a) $p = 1$.



(b) $p = 1/5$.

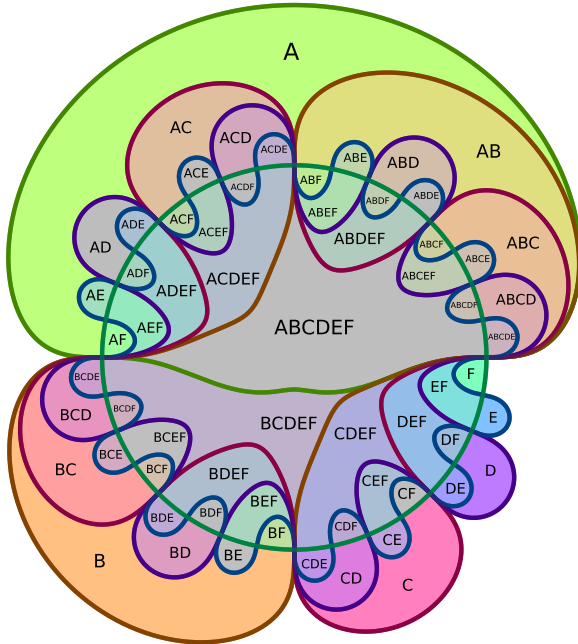
Figure 5: Linear decay on the sinusoidal Smith diagram.

Instead of linear decay we can bring back the exponential decay, but with a base $1/2 < b < 1$:

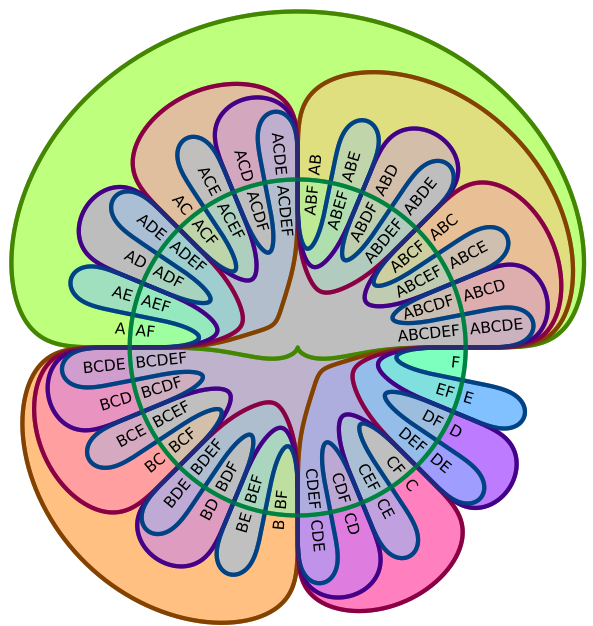
$$\lambda(i) = b^{i+\varepsilon}, \quad i = 0, 1, \dots, n-2, \quad (4)$$

$$\lambda(n-1) = 0. \quad (5)$$

If the shape parameter p is small enough, then as we increase b , we create more space for text labels around the circle (Figure 6b). Here $\lambda(n-1) = 0$ keeps the last boundary the $y = 0$ line, which is mapped to the unit circle by the projection. Additionally, $\varepsilon > 0$ ensures that $f_i(x) < 1$, and we do not cross the origin when projecting. In practice, we can use $\varepsilon = 0$, or even $\varepsilon \gg 0$ to adjust the appearance of the inside of the projected diagram.



(a) Linear decay, $p = 1/3$.



(b) $b = 4/5, p = 1/5$.

Figure 6: Sinusoidal *VennFan* diagrams for $n = 6$ with linear and modified exponential decay.

An arguably more visually pleasing alternative to the modified exponential amplitude decay is to modify the linear decay as:

$$\lambda_{\delta, \varepsilon}(i) = \frac{\delta + \varepsilon - 1}{n-2}i - \varepsilon + 1, \quad i = 0, 1, \dots, n-2, \quad (6)$$

$$\lambda_{\delta, \varepsilon}(n-1) = 0. \quad (7)$$

Here δ controls the size of the smallest “fan blades”, and ε the size of the first step we take in the amplitude decay process. In case of the basic linear decay ($\lambda(i) = \frac{n-1-i}{n}$), these parameters were the same: $\delta = \varepsilon = 1/n$.

Instead of sine functions, we can also use cosines to form a Venn-like diagram [15]. Here we can also apply alternative scaling after shaping the curves (Equation 8, Figure 7a). We use $x \in [2\pi, 4\pi]$ (as opposed to $x \in [0, 2\pi]$) to preserve the left-to-right order in which the sets are drawn. The resulting *VennFan* diagram turns out to be a planar rendering of Edwards’ cogwheel construction; the resemblance is especially clear with linear scaling (Figure 7b).

$$f_i(x) = \lambda(i) \operatorname{sgn}(\cos(2^{i-1}x)) |\cos(2^{i-1}x)|^p, \quad x \in [2\pi, 4\pi], \quad i = 0, 1, \dots, n-1. \quad (8)$$

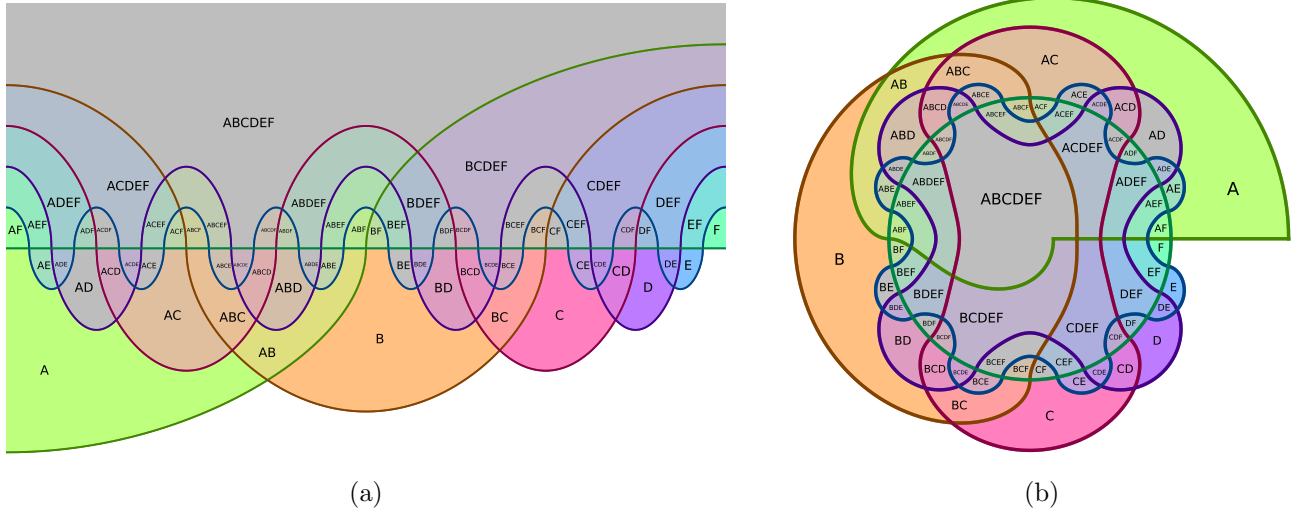


Figure 7: Cosine-based Venn-like diagram with linear scaling (a) and its projection (b) with $p = 1/2$.

3.1 Empirical Properties

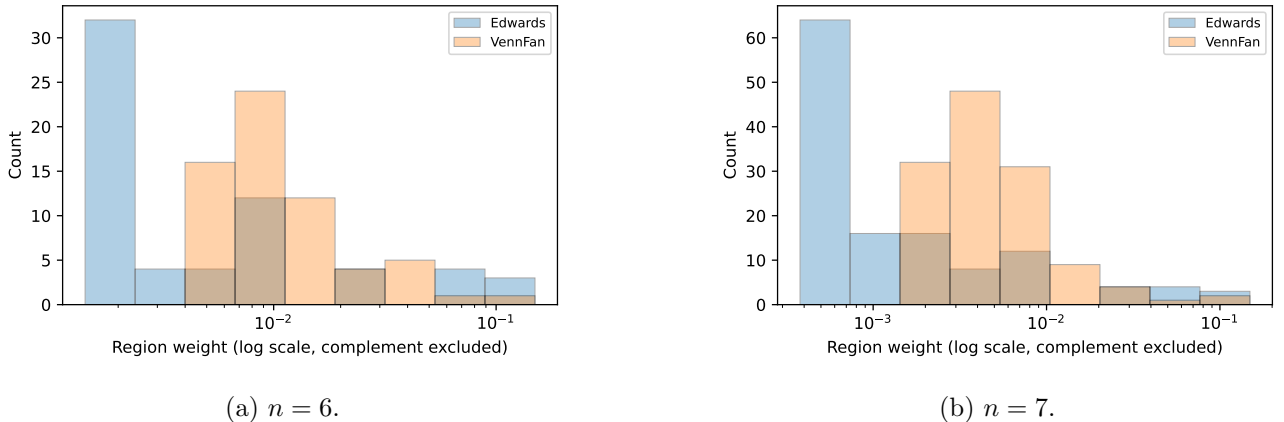
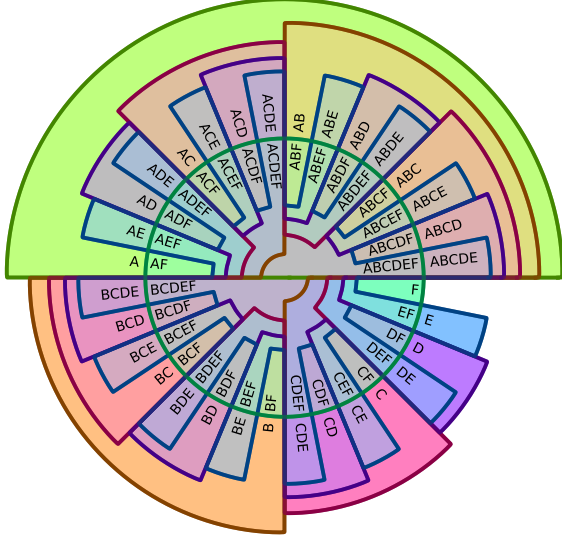


Figure 8: Histograms of normalized region areas (weights) for Edwards’ cogwheel diagram and cosine-based *VennFan* (modified linear amplitude decay $p = 1/5$, $\delta = 1/3$, $\varepsilon = 1/9$).

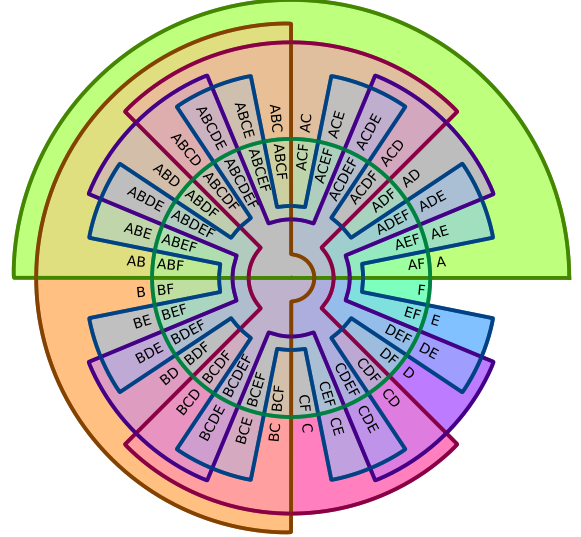
A major limitation of classical constructions for large n is that the areas of the regions shrink rapidly, which makes it difficult to place readable labels. To quantify this effect, in Figure 8 we compare the normalized region-area distributions of Edwards’ cogwheel diagram and the cosine-based *VennFan*. Although the two diagrams are topologically equivalent, the *VennFan* construction produces a noticeably less extreme spread of region sizes, making it a more data-friendly planar realization of the same combinatorial structure. To obtain accurate region areas for Edwards’ diagram we reimplemented

his original spherical construction and its stereographic projection (Appendix A). In principle, by pushing the parameters of *VennFan* to extreme values (e.g. p close to zero and λ close to one), the region areas can be made nearly equal. For a more realistic comparison, however, we report results for moderate parameter choices that preserve the overall look of the diagrams.

One advantage of the *VennFan* construction is the ability to adjust parameters to obtain diagrams with different visual styles. For example, at very small p we get a less rounded version of the diagram (Figure 9). Arguably, this makes the sine-based version harder to parse, since it is not a simple diagram in the first place, and extremely small p values exaggerate this.



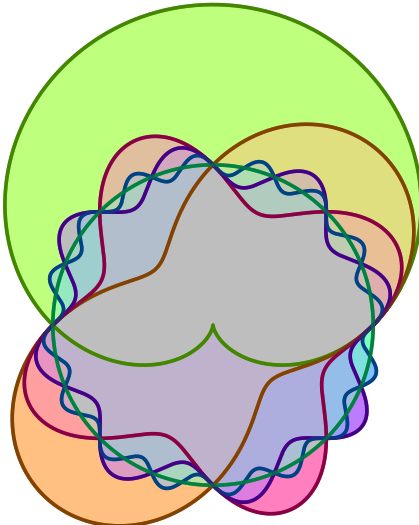
(a) Sine-based.



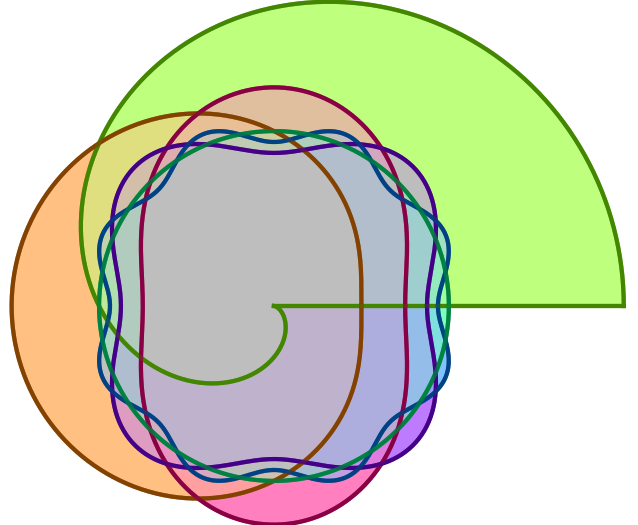
(b) Cosine-based.

Figure 9: $n = 6$, $p = 1/1000$, $b = 5/6$.

Finally, to reiterate the importance of these modifications, in Figure 10 we show the projection of the classical trigonometric constructions. They look beautiful, but they are not really suitable for representing data.



(a) Sine-based.



(b) Cosine-based.

Figure 10: *VennFan* constructions from unshaped sinusoids $n = 6$, $p = 1$, $b = 1/2$.

3.2 Theoretical Remarks

The radial projection step preserves the topology of the regions. Intuitively, as long as the base curves f_i form a valid diagram on the strip $[-\pi, \pi] \times [-1, 1]$ (or $[2\pi, 4\pi] \times [-1, 1]$ for the cosine version) and we choose parameters such that $1 + f_i(\vartheta) > 0$ for all i, ϑ , the curves $g_i(\vartheta)$ simply wrap the strip around the circle without tearing or gluing. Consequently, the intersection pattern of the curves and the topological completeness of the Venn diagram is preserved by the projection.

The cosine family we start from is an explicit trigonometric realization of Edwards' construction [4, 5, 15], which is known to produce simple n -Venn diagrams (no triple intersections) both on the sphere and, after projection, in the plane [7, 11]. Hence the unmodified cosine construction underlying *VennFan* is simple. The cosine-based *VennFan* with alternate scaling is often simple in practice, but this depends on the parameters (e.g. p and the amplitude decay) and is not guaranteed a priori. Moreover, the first boundary in the cosine construction ($\cos(x/2)$) does not complete a full period on $x \in [2\pi, 4\pi]$, and its projection does not form a closed curve. This can be remedied by connecting $g_0(2\pi)$ and $g_0(4\pi)$ with a straight line segment.

The sine-based *VennFan* construction is not simple in general, and the curves may intersect more often than in the unmodified Smith construction, yielding an independent family rather than a strict Venn diagram. However, for visualization purposes this is often not a practical issue: the boundaries are drawn with nonzero stroke width, and for aesthetically chosen parameters the extra tiny regions tend to be covered by the boundaries, so the rendered image is effectively a Venn diagram.

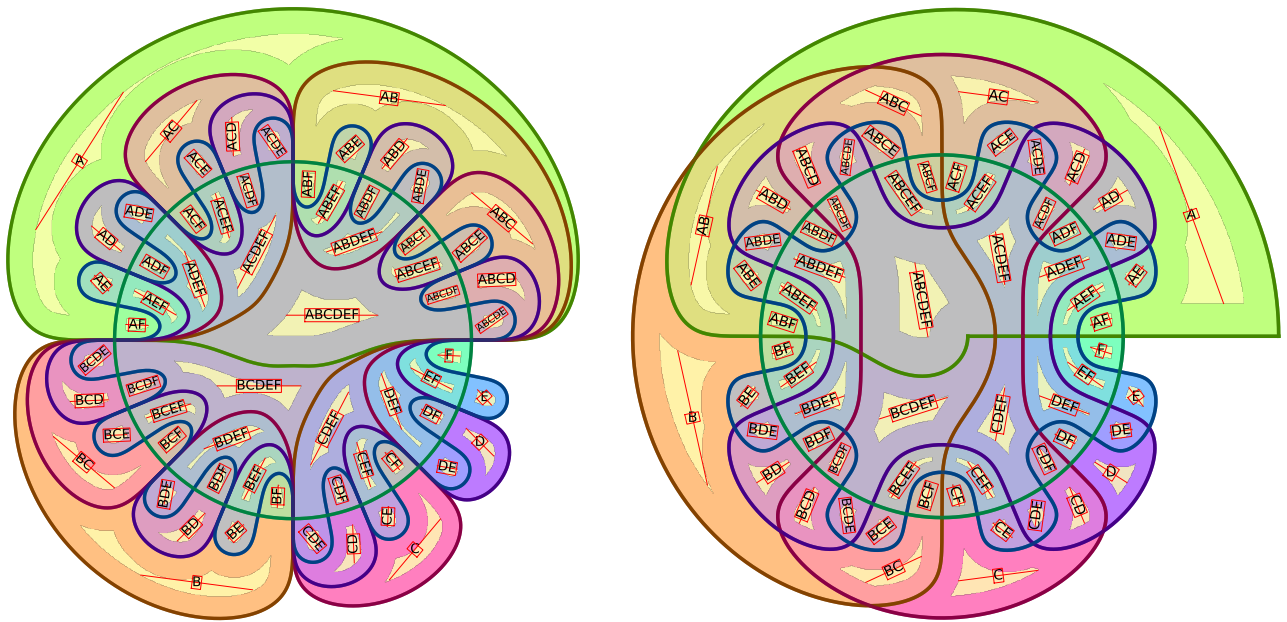
4 Label placement

An important aspect of readable Venn diagrams is the placement of region labels. In *VennFan*, we use two complementary strategies: radial labels placed near the unit circle, and labels placed by a geometric heuristic. The first option is to place labels around the projection circle in the angular order induced by the construction. As x increases, the sign vector $(\text{sgn } \sin(2^0 x), \dots, \text{sgn } \sin(2^{n-1} x))$ changes by flipping exactly one coordinate at a time, yielding the binary-reflected Gray code order on $\{0, 1\}^n$; this provides a principled circular ordering of the 2^n regions for radial labels [13]. For larger n , a balanced approach would be to use radial placement for some regions and the visual-center heuristic for others.

We also consider defining and approximating an “optimal” text placement method inside each region. A straightforward heuristic would be to use the geometric center or *centroid* of the region. For non-convex regions this can yield poor results: the centroid may lie very close to the boundary or even outside the region. A better heuristic is to place labels at points that approximate the *visual center* of each region. Intuitively, the visual center is the point that “looks most centered” while remaining well separated from the boundary, and can be defined as the center of a largest inscribed disk in the region [6]. By standard compactness arguments, such a maximizer exists for every bounded region with nonempty interior. In practice we approximate it numerically (for example, using sampling or a distance transform on a rasterization of the diagram) and use this point as the anchor for the region’s text label.

A limitation of the visual-center heuristic is that text labels are not point-like objects: they have width and height, and orientation matters. Simply placing the label at the visual center ignores rotation and can fail to maximize the readable font size. A more refined objective is to find an anchor point and a text rotation that maximize the font size for which the label still fits inside the region.

We approximate this objective with the following heuristic. First, we erode the region until its area is reduced to a fixed fraction of its original area; this shrinks the region inward and creates a margin. On this eroded region we then look for the longest line segment that fits entirely inside it. In practice, we approximate this by taking the visual center of the eroded region and sampling line directions through it, keeping the longest segment that remains inside. Finally, we place the label at the midpoint of this segment and rotate the text to align with the segment direction. This produces labels that are visually centered in a more robust sense and can be rendered at larger font sizes without touching the boundary. Figure 11 shows the steps of this heuristic for $n = 6$, and Figures 12 and 13 illustrate the resulting label placements for $n = 7$.



(a) Sine-based.

(b) Cosine-based.

Figure 11: *VennFan* label placement heuristic $n = 6$, $p = 1/5$, $\delta = 1/4$, $\varepsilon = 1/7$.

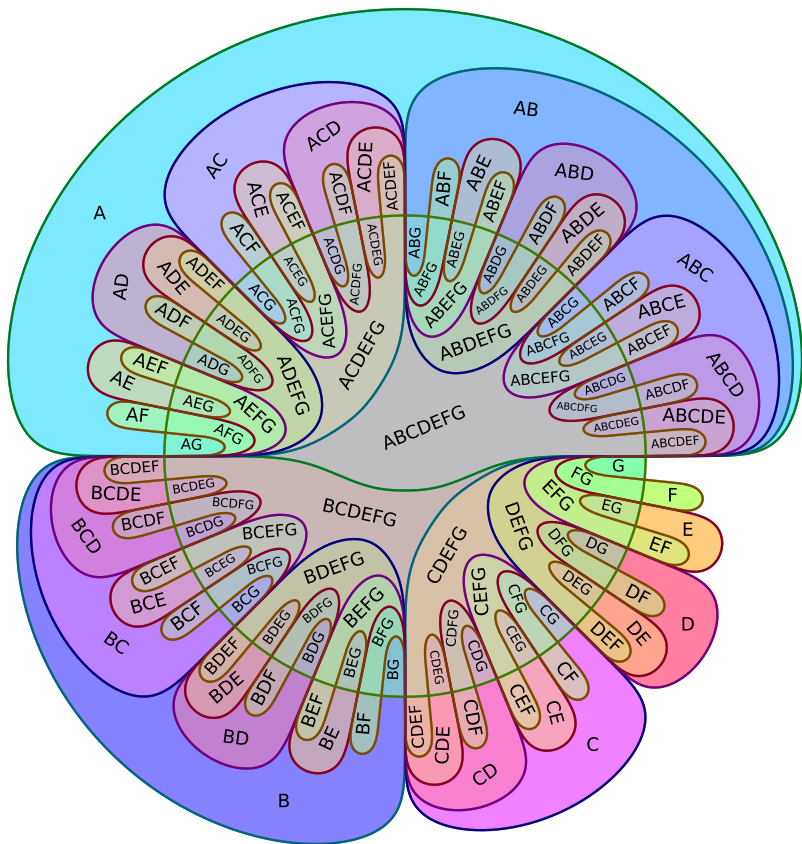


Figure 12: Sine-based *VennFan* $n = 7$, $p = 1/7$, $\delta = 1/4$, $\varepsilon = 1/7$.

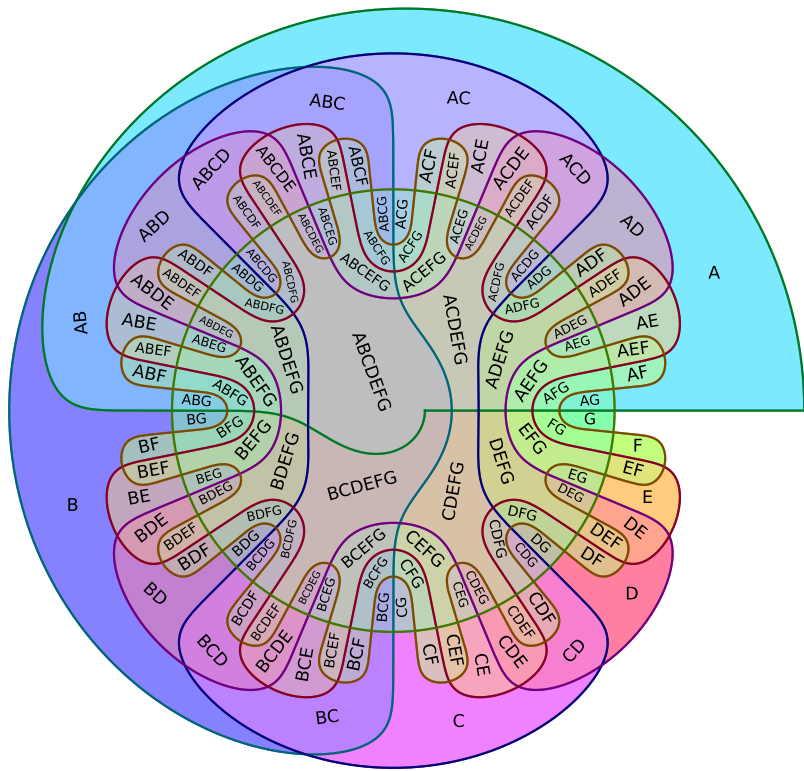


Figure 13: Cosine-based *VennFan* $n = 7$, $p = 1/7$, $\delta = 1/4$, $\varepsilon = 1/7$.

5 Conclusions

We presented *VennFan*, a family of n -set Venn diagrams obtained from shaped trigonometric curves by polar coordinate projection to the disc. We replaced the exponential amplitude decay of Smith’s construction by tunable decay schemes and obtained closed, fan-shaped curves. In the cosine-based variant, we recover a planar diagram that is topologically equivalent to Edwards’ cogwheels, but with more direct geometric control. For suitable parameter choices, the resulting diagrams remain practically readable for n up to about 8. The accompanying Python implementation exposes the underlying parameters, allowing users to adjust the trade-off between visual styles to fit their specific use cases.

Declaration on Generative AI

During the preparation of this manuscript, OpenAI's ChatGPT-5 was used to assist with grammar, paraphrasing, rewording, and targeted code review and augmentation. All AI-assisted outputs were subsequently reviewed, edited, and, where applicable, validated, and we assume full responsibility for the content of the publication.

Acknowledgements

Supported by the EKÖP-25 University Research Scholarship Program of the Ministry for Culture and Innovation from the source of the National Research, Development and Innovation Fund.

Additional support by the Hungarian National Research, Development and Innovation Office within the framework of the Thematic Excellence Program 2021 – National Research Sub programme: “Artificial intelligence, large networks, data security: mathematical foundation and applications” and the Artificial Intelligence National Laboratory Program (MILAB).

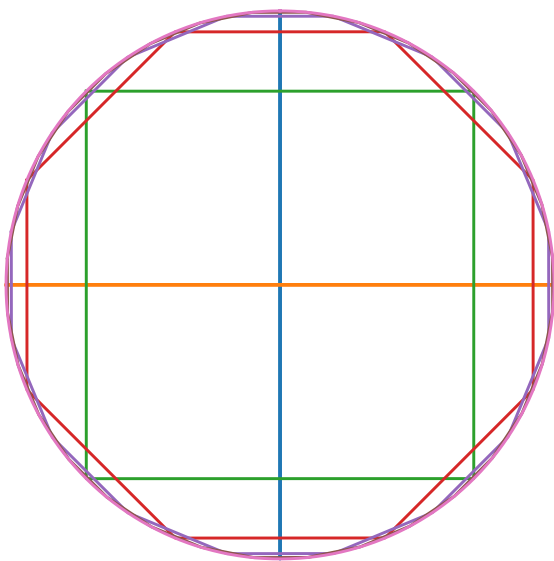
We would like to express our gratitude to András Lukács for his valuable consultation. We would also like to thank GitHub for providing us academic access.

References

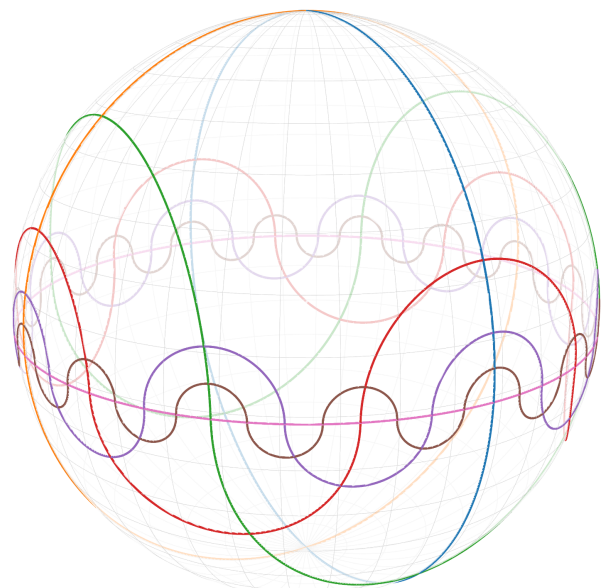
- [1] Jeremy Carroll, Frank Ruskey, and Mark Weston. Which n -Venn diagrams can be drawn with convex k -gons? *Discrete & Computational Geometry*, 37(4):619–628, 2007.
- [2] Jeremy J Carroll. Drawing Venn Triangles. *HP Laboratories Technical Report HPL*, (73), 2000.
- [3] Anthony Edwards. Venn diagrams for many sets. *New Scientist*, 121(1646):51–56, 1989.
- [4] Anthony William Fairbank Edwards. *Cogwheels of the mind: the story of Venn diagrams*. JHU Press, 2004.
- [5] AWF Edwards and CAB Smith. New 3-set Venn diagram. *Nature*, 339(6222):263, 1989.
- [6] Daniel Garcia-Castellanos and Umberto Lombardo. Poles of inaccessibility: A calculation algorithm for the remotest places on earth. *Scottish Geographical Journal*, 123(3):227–233, 2007.
- [7] Mohammad Farrokhi Derakhshandeh Ghouchan. Fully reducible simple Venn diagrams, 2022.
- [8] Branko Grünbaum. Venn diagrams I. *Geombinatorics*, 1(4):5–12, 1992.
- [9] Branko Grünbaum. Venn diagrams II. *Geombinatorics*, 2(2):25–32, 1992.
- [10] Branko Grünbaum. Venn diagrams and independent families of sets. *Mathematics Magazine*, 48(1):12–23, 1975.
- [11] Khalegh Mamakani and Frank Ruskey. Simple Spherical Venn diagrams with Isometry Groups of Order Eight.
- [12] Frank Ruskey and Mark Weston. A Survey of Venn Diagrams. *The Electronic Journal of Combinatorics*, 2005.
- [13] Carla Savage. A survey of combinatorial Gray codes. *SIAM review*, 39(4):605–629, 1997.
- [14] John Venn. I. On the diagrammatic and mechanical representation of propositions and reasonings. *The London, Edinburgh, and Dublin Philosophical Magazine and Journal of Science*, 10(59):1–18, 1880.
- [15] Mark Richard Nicholas Weston. *Symmetries of Venn diagrams on the sphere*. PhD thesis, 2009.
- [16] Yingdan Yuan, Jiajia Zuo, Hanyue Zhang, Mengting Zu, Maoyun Yu, and Sian Liu. Transcriptome and metabolome profiling unveil the accumulation of flavonoids in *Dendrobium officinale*. *Genomics*, 114(3):110324, 2022.

A Recreating Edwards' Cogwheel Diagrams

Edwards' Venn diagrams are based on a spherical construction. A convenient way to describe the construction is via prisms with regular 2^k -gonal bases whose side faces intersect the sphere in circles. Figure 14a shows these bases as they appear under orthogonal projection onto the equatorial disk. On the sphere there are three distinguished circles: the equator and two mutually orthogonal longitudes. In the equatorial projection these become one circle and two line segments (diameters). Each 2^k -gonal prism intersects the sphere in 2^k circles; from these we select northern and southern semicircles in alternating order around the polygon. Together with the equator and the two longitudes, these arcs form a simple n -set Venn diagram on the sphere (Figure 14b). Finally, stereographic projection of this spherical configuration yields the planar cogwheel diagrams of Edwards: Figure 15a shows the canonical variant, while Figure 15b shows the “inside-out” variant where the topological equivalence with *VennFan* is more apparent.

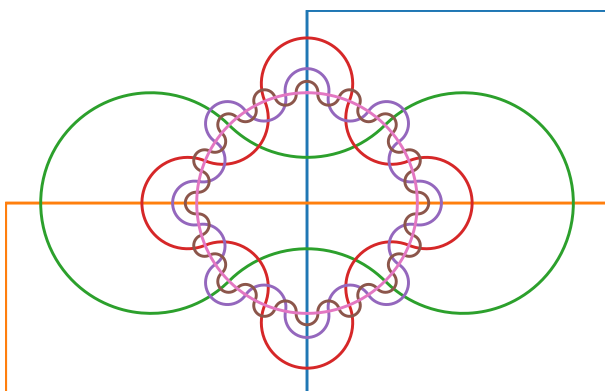


(a) Equatorial projection of the curves (prism bases).

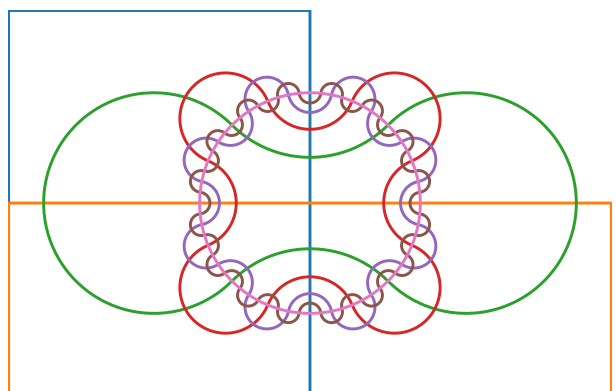


(b) Edwards' Venn diagram on the sphere.

Figure 14: Edwards' spherical Venn diagram and its equatorial projection ($n = 7$).



(a) Projection onto a plane below the sphere.



(b) Projection onto a plane above the sphere.

Figure 15: Edwards' cogwheel Venn diagram obtained by stereographic projection ($n = 7$).

B Additional *VennFan* diagrams

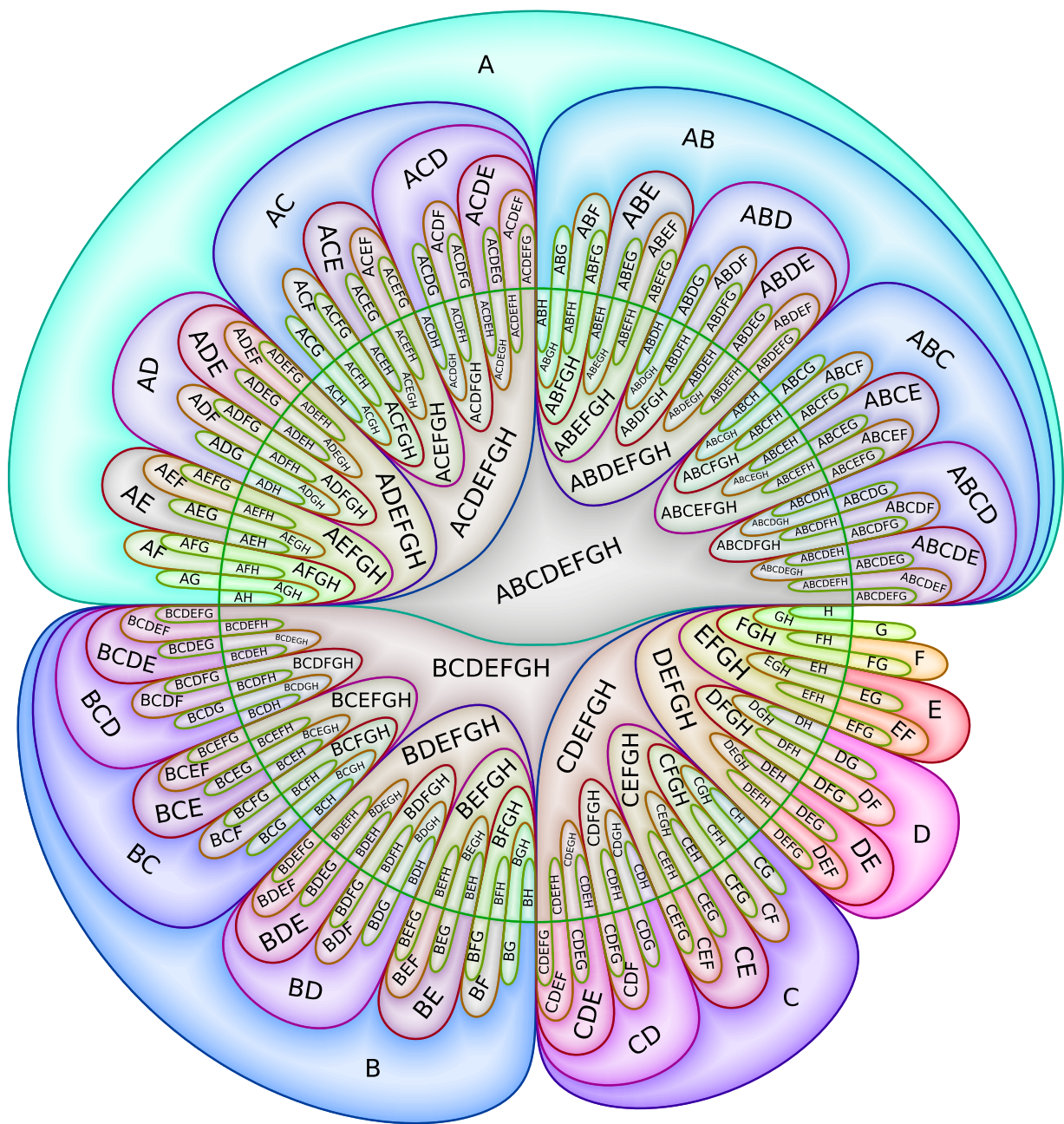


Figure 16: Sine-based *VennFan* $n = 8$, $p = 1/7$, $\delta = 1/5$, $\varepsilon = 1/8$.

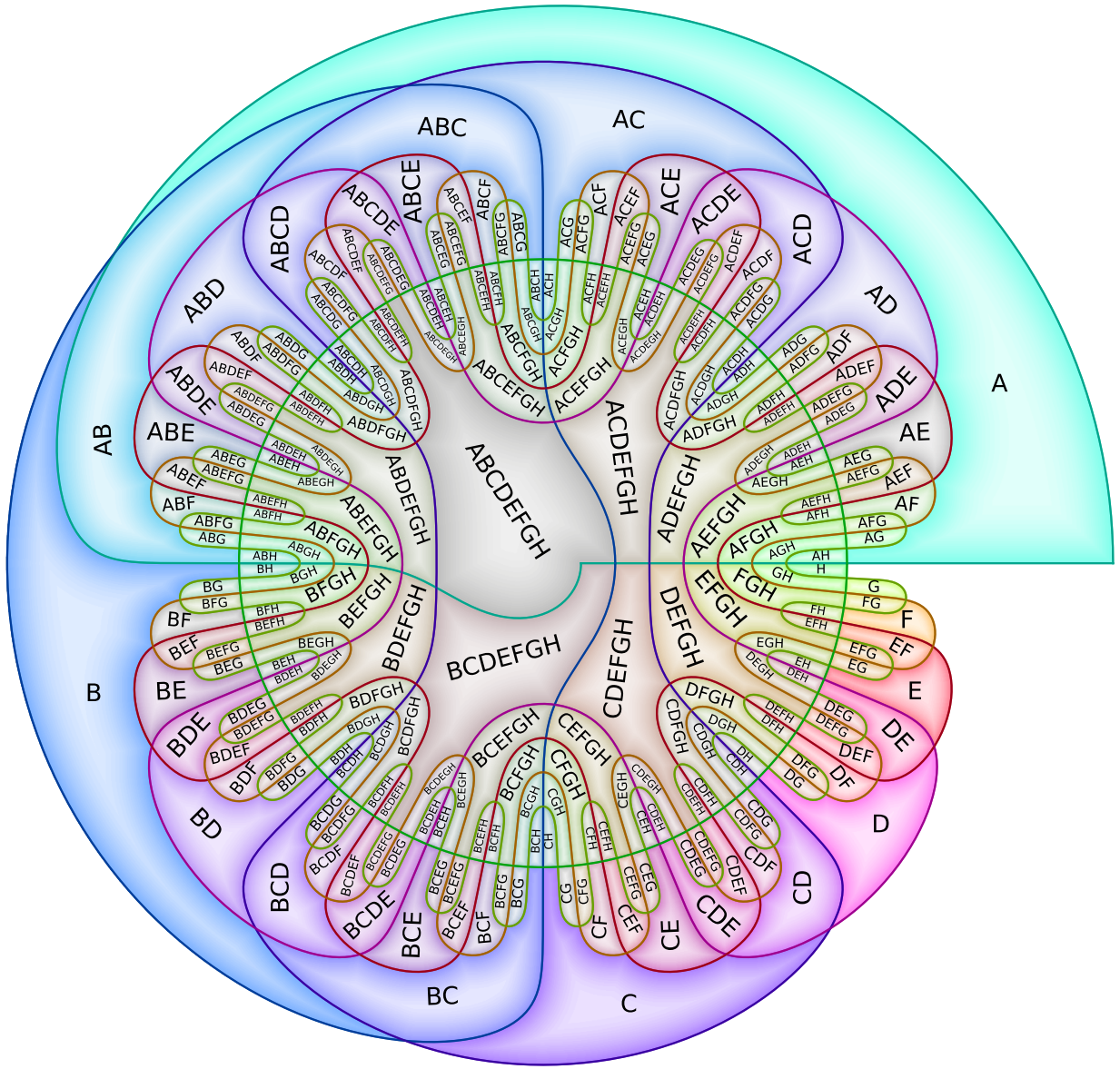


Figure 17: Cosine-based *VennFan* $n = 8$, $p = 1/7$, $\delta = 1/5$, $\varepsilon = 1/8$.

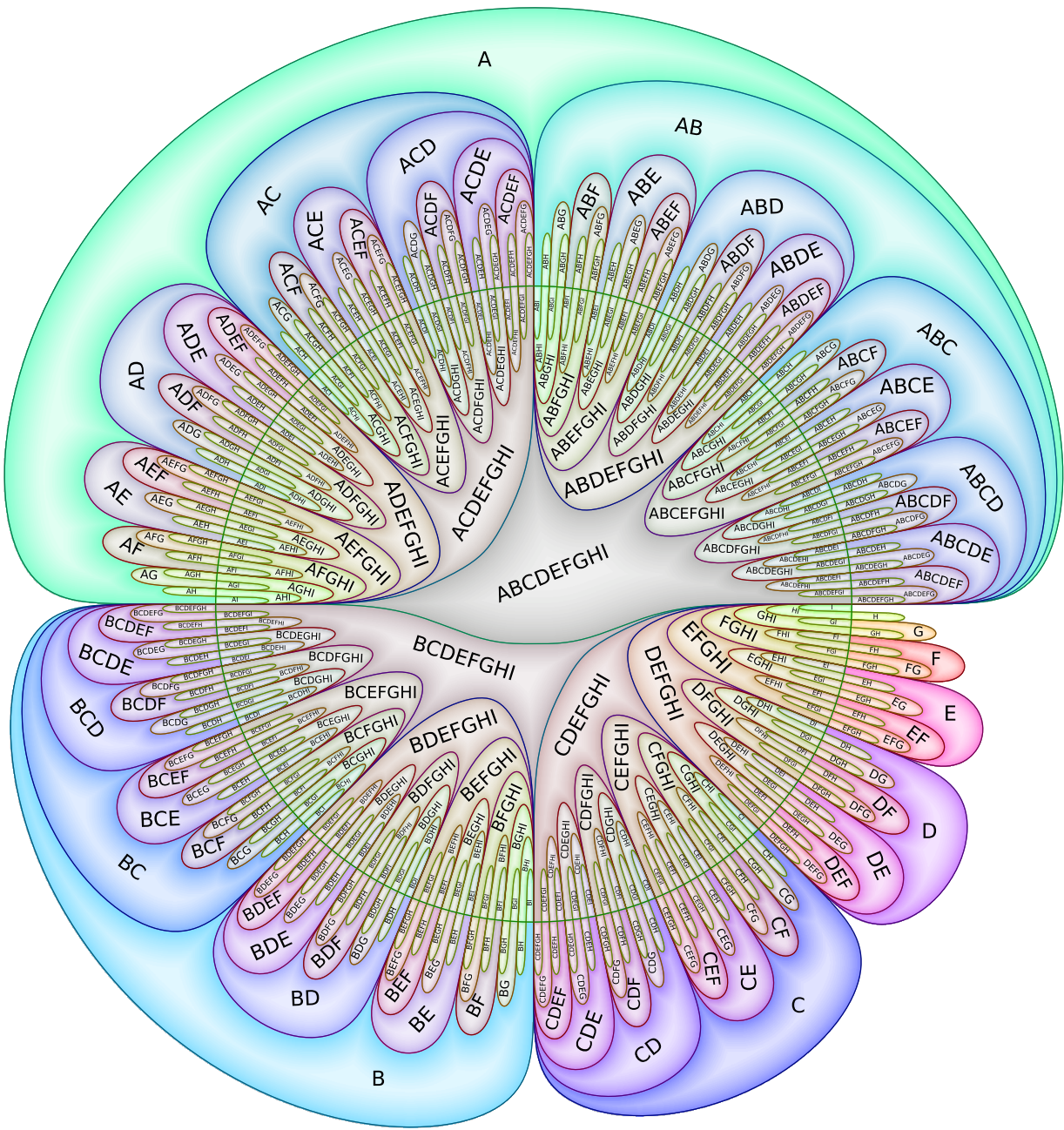


Figure 18: Sine-based *VennFan* $n = 9$, $p = 1/7$, $\delta = 1/6$, $\varepsilon = 1/8$.

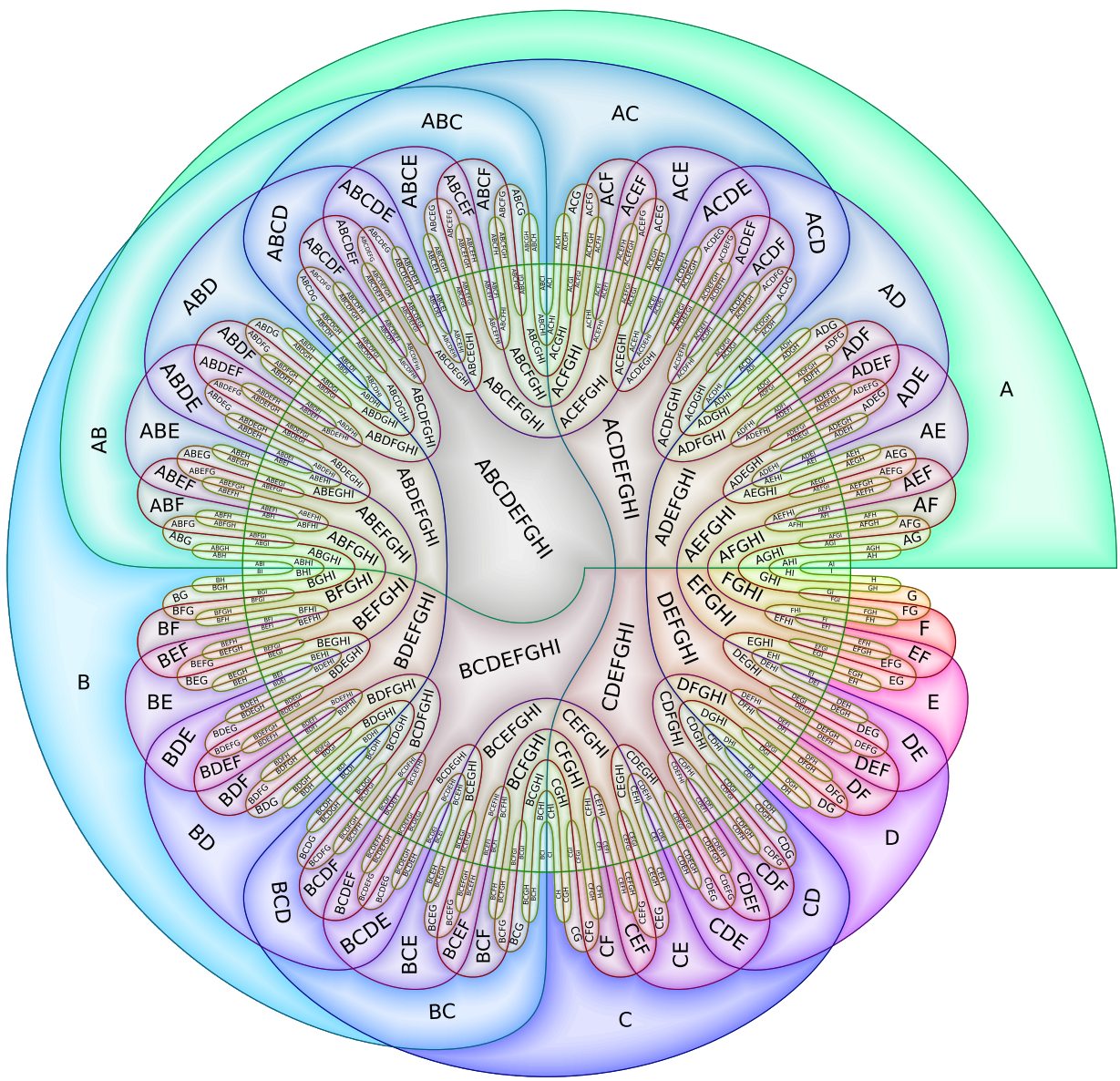


Figure 19: Cosine-based *VennFan* $n = 9$, $p = 1/7$, $\delta = 1/6$, $\varepsilon = 1/8$.